Free Convection Flow of Newtonian Fluid along a Vertical Plate Embedded in a Double Layer Porous Medium*

Nabil BEITHOU**, Hikmet S. AYBAR***
Kahraman ALBAYRAK**** and Ozan ERENAY***

Porous medium has got a great interest especially in the recent years, for its wide application in geophysics, petroleum, and air conditioning. Many studies related to porous medium were performed, and most of them are dealing with constant porosity. For the fact that porosity is non-uniform, a great concern has been directed toward the variable porosity studies. In this study, the effects of a double layer porous medium on the free convection along vertical plate embedded in this porous medium were investigated. The governing partial nonlinear differential equations were transformed into a set of ordinary differential equations, which have been solved by the fourth-order Runge-Kutta method. The results are obtained for different layer permeability K, and layer length, L. One case is compared with the previous study, and the result is found to be in good agreement with the result of previous study. Results show that permeability ratios greater than one tend to increase in Nusselt number, and it is valuable to use a high permeability ratio layer in the range of 0.2η to get higher heat transfer rate instead of using constant permeability medium.

Key Words: Variable Permeability, Natural Convection, Porous Medium

1. Introduction

Porous medium has got great interest in the recent years because of its wide practical applications in geophysics, thermal insulation of buildings, petroleum resources, packed bed reactors, and sensible heat storage beds. Many studies (e.g. Refs.(1) through (5)) have been done to investigate free convection heat transfer from a plate with different geometry embedded in a porous medium saturated by Newtonian and non-Newtonianfluids. All of these studies have dealt with a single layer porous medium with a uniform averaged porosity. The variation of the porosity is the fact in most of the real porous medium. If the variation of the porosity is taken into consideration, a better description of the temperature distribution and velocity field will be obtained.

In this study, the free convection flow of a Newtonian fluid along a vertical plate embedded in a double layer porous medium has been investigated in two cases: constant wall temperature, and constant heat flux. The considered porous media has two porous layers with different permeability. The Fig. 1 shows the illustration of the problem. The vertical plate is touching the first layer with the permeability of K_1, and the second layer with permeability of K_2 fills the rest of the space. The effects of two parameters on the free convection from the vertical plate have been analyzed. Those parameters are the thickness of the first layer, and the permeability ratio of the layers. The permeability is independent of the nature of the fluid but it depends on the geometry of the medium. Thus, the permeability K is function of porosity and particle diameter[6]. The effective (overall) thermal conductivity of porous medium is function of the porosity, and thermal conductivity of fluid and solid. It is assumed that the porosity of the layers does not change. The permeability of layers varies because of the change of particle diameter. Since the porosity of layers does not change, the effective

* Received 24th January, 2000
** School of Engineering, Cyprus International University, Lefkosa, KKTC, Mersin 10 Turkey
*** Department of Mechanical Engineering, Eastern Mediterranean University, G. Magosa, KKTC, Mersin 10 Turkey. E-mail: hikmet.aybar@emu.edu.tr
**** Department of Mechanical Engineering, Middle East Technical University, Ankara, Turkey

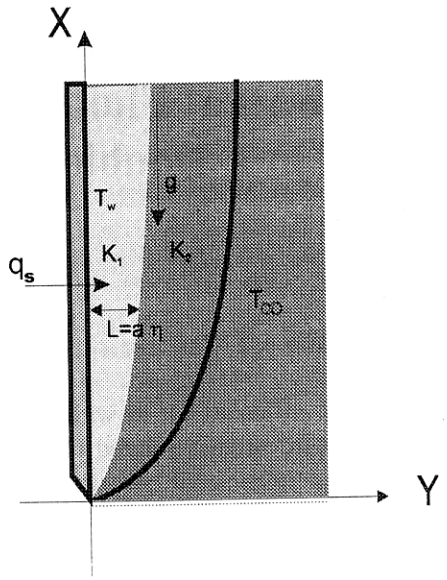

Fig. 1 Schematic diagram for the vertical plate with two porous layers

thermal conductivity of the layers does not change either. The similarity solution method has been used to solve the governing equations.

Nomenclature

a : constant
f : dimensionless stream function
g : gravitational acceleration
h : local heat transfer coefficient
K : bed permeability
k_m : thermal conductivity of the fluid saturated porous medium.
l : length of the plate
L : dimensionless length of the inserted layer
p : pressure
Ra : Rayleigh number
T : temperature
q : heat flux
u : velocity in x-direction
v : velocity in y-direction
x : transverse coordinate
y : longitudinal coordinate

Greek symbols

α : equivalent thermal diffusivity
β : coefficient of thermal expansion
η : dimensionless similarity variable
μ : dynamic viscosity
θ : dimensionless similarity variable
ρ : density
ψ : stream function

Subscripts

w : wall
∞ : infinity
1, 2 : first and second layers

Superscripts

* : dimensionless property

2. Governing Equations

The problem is illustrated by Fig. 1. It represents a vertical plate embedded in a double-layer porous medium, and each porous layer has different permeability. The governing equations, continuity and energy equations, for this problem can be written as[6]

$$\frac{\partial u}{\partial x}+\frac{\partial v}{\partial y}=0 \tag{1}$$

$$u\frac{\partial T}{\partial x}+v\frac{\partial T}{\partial y}=\alpha\frac{\partial^2 T}{\partial y^2} \tag{2}$$

The momentum equation in the x direction can be written using Darcy's Law[6] with gravitational term for natural convection as

$$u=-\frac{K}{\mu}\left[\frac{\partial p}{\partial x}+\rho g\right] \tag{3}$$

Out side the boundary layer, the flow remains stagnant, which gives

$$-\left(\frac{\partial p}{\partial x}\right)=\rho_\infty g \tag{4}$$

In this problem, it is assumed that Boussinesq[6] approximation is valid, which is

$$\rho=\rho_\infty[1-\beta(T-T_\infty)] \tag{5}$$

As it is mentioned above, the cases of constant temperature and constant heat flux have been investigated. The boundary conditions and solutions of the equations are given in the following sections.

2.1 Constant wall temperature

The governing equations (i.e. Eqs. (1)-(3)) are being applicable for both layers. The boundary conditions for these equations are

$$v_1=0,\quad T=T_w \quad \text{at } y=0 \tag{6}$$

$$u_2=0,\quad v_2=0,\quad T=T_\infty \quad \text{at } y\to\infty \tag{7}$$

$$\frac{\partial u_1}{\partial y}=\frac{\partial u_2}{\partial y} \quad \text{at } y=L \tag{8}$$

To simplify the equations the following dimensionless terms have been introduced[2]

$$x^*=\frac{x}{l},\quad y^*=\frac{y}{l} \tag{9}$$

$$u^*=\frac{u}{\left[\rho_\infty\beta g K_2\dfrac{(T_w-T_\infty)}{\mu}\right]},$$

$$v^*=\frac{v}{\left[\rho_\infty\beta g K_2\dfrac{(T_w-T_\infty)}{\mu}\right]} \tag{10}$$

$$T^*=\frac{(T-T_\infty)}{(T_w-T_\infty)} \tag{11}$$

$$Ra^*=\left[\rho_\infty\beta g K_2\frac{(T_w-T_\infty)}{(\mu\alpha)}l\right] \tag{12}$$

Applying the Eqs. (4) and (5) into the Eq. (3) and using the dimensionless terms, the governing equations for both layers can be written as

$$\frac{\partial u_1^*}{\partial x^*}+\frac{\partial v_1^*}{\partial y^*}=0 \tag{13}$$

$$\frac{\partial u_2^*}{\partial x^*}+\frac{\partial v_2^*}{\partial y^*}=0 \tag{14}$$

$$u_1^*=\left(\frac{K_1}{K_2}\right)T^* \tag{15}$$

$$u_2^*=T^* \tag{16}$$

$$u_1^*\frac{\partial T^*}{\partial x^*}+v_1^*\frac{\partial T^*}{\partial y^*}=\frac{1}{Ra^*}\frac{\partial^2 T^*}{\partial y^{*2}} \tag{17}$$

$$u_2^*\frac{\partial T^*}{\partial x^*}+v_2^*\frac{\partial T^*}{\partial y^*}=\frac{1}{Ra^*}\frac{\partial^2 T^*}{\partial y^{*2}} \tag{18}$$

To transform the non-linear partial differential equations into a set of ordinary differential equations the following dimensionless similarity variables are defined

$$\xi(x^*)=\left(\frac{x^*}{Ra^*}\right)^{1/2} \tag{19}$$

$$\eta=\left(\frac{y^*}{\xi(x^*)}\right)=y^*\left(\frac{Ra^*}{x^*}\right)^{1/2} \tag{20}$$

$$\psi=U(x^*)\xi(x^*)f(\eta)=\left(\frac{x^*}{Ra^*}\right)^{1/2}f(\eta) \tag{21}$$

Using the new defined variables, the velocity components become

$$u_1^*=u_2^*=u^*=\frac{\partial\psi}{\partial y^*}=f'(\eta) \tag{22}$$

$$v_1^*=v_2^*=v^*=-\frac{\partial\psi}{\partial x^*}=\frac{\frac{1}{2}(f'\eta-f)}{(Ra^*x^*)^{1/2}} \tag{23}$$

Then, the Eqs.(13)-(18), and their boundary conditions become

$$\theta=\left(\frac{K_1}{K_2}\right)f', \quad \text{where } 0<\eta<L \tag{24}$$

$$\theta=f', \quad \text{where } \eta>L \tag{25}$$

$$\theta''+\frac{1}{2}\theta' f=0, \text{ for all } \eta \tag{26}$$

and their the boundary conditions become

$$\theta=1,\ f=0 \text{ at } \eta=0 \tag{27}$$

$$\theta=0,\ f'=0 \text{ at } \eta\to\infty \tag{28}$$

The local heat flux at the wall is

$$q_w=-k_m\left(\frac{\partial T}{\partial y}\right)_{y=0}$$

$$=-k_m(T_w-T_\infty)\theta'(0)\frac{1}{l}\left(\frac{Ra^*}{x^*}\right)^{1/2} \tag{29}$$

and the local Nusselt number is given as

$$Nu_x=\frac{hx}{k_m}=\frac{q_w x}{k_m(T_w-T_\infty)} \tag{30}$$

Substituting the Eq.(30) into Eq.(29) gives

$$\frac{Nu_x}{\left(\frac{Ra^*}{x^*}\right)^{1/2}}=-\theta'(0) \tag{31}$$

2.2 Constant heat flux

The problem represented in Fig. 1 has been analyzed in case of constant heat flux. The continuity, energy and momentum equations are given in Eqs. (1), (2) and (3), respectively. The Eqs.(1), (2), and (3) are applicable for both layers. The boundary conditions for that case are

$$v_1=0, \quad \frac{\partial T}{\partial y}=-\frac{q_w}{k} \quad \text{at } y=0 \tag{32}$$

$$u_2=0, \quad v_2=0, \quad T=T_\infty \quad \text{at } y\to\infty \tag{33}$$

$$\frac{\partial u_1}{\partial y}=\frac{\partial u_2}{\partial y} \quad \text{at } y=L \tag{34}$$

To simplify the equations, the following dimensionless terms have been introduced,

$$x^*=\frac{x}{l},\ y^*=\frac{y}{l},\ u^*=\frac{u}{\left(\frac{\alpha}{l}\right)},\ v^*=\frac{v}{\left(\frac{\alpha}{l}\right)},$$

$$\text{and } T^*=\frac{\rho g\beta K_2 L(T-T_\infty)}{\mu\alpha} \tag{35}$$

Using these dimensionless terms, the continuity and momentum equations (i.e. Eqs.(1) and (3)) can be written as in Eqs.(13) through (16) for both layers, and the energy equations for both layers can be written as,

$$u_1^*\frac{\partial T^*}{\partial x^*}+v_1^*\frac{\partial T^*}{\partial y^*}=\frac{\partial^2 T^*}{\partial y^{*2}} \tag{36}$$

$$u_2^*\frac{\partial T^*}{\partial x^*}+v_2^*\frac{\partial T^*}{\partial y^*}=\frac{\partial^2 T^*}{\partial y^{*2}} \tag{37}$$

To transform the nonlinear partial differential equations above into a set of ordinary differential equations, the following stream function and dimensionless similarity variables[4] are defined

$$\eta=x^{*-1/3}y^* \tag{38}$$

$$\psi=x^{*2/3}f(\eta) \tag{39}$$

$$T^*=x^{*1/3}\theta(\eta) \tag{40}$$

By using these dimensionless variables, the dimensionless governing equations have been reduced to a system of ordinary differential equations which are

$$\theta=\left(\frac{K_1}{K_2}\right)f', \quad \text{where } 0<\eta<L \tag{41}$$

$$\theta=f', \quad \text{where } \eta>L \tag{42}$$

$$\theta''+\frac{2}{3}\theta' f-\frac{1}{3}f'\theta=0, \text{ for all } \eta \tag{43}$$

with the boundary conditions

$$\theta=1,\ f=0 \text{ at } \eta=0 \tag{44}$$

$$\theta=0,\ f'=0 \text{ at } \eta\to\infty \tag{45}$$

and the expression for the dimensionless excess surface temperature is given by

$$T_w^*=\theta(0) \tag{46}$$

3. Results and Discussion

The governing equations and its boundary conditions have been nondimensionalized, then solved using the similarity method, and the resulted equations with the boundary conditions solved numerically using the fourth order Runge-Kutta method for both cases. As it is mentioned in the Refs.(3) and (4), the boundary condition ($\eta\to\infty$) is replaced by a large value of η in our study as well. In our analysis, for the case of constant surface temperature the boundary condition is replaced by $\eta=9$ and for the case of constant heat flux is replaced by $\eta=12$. Those values of η were

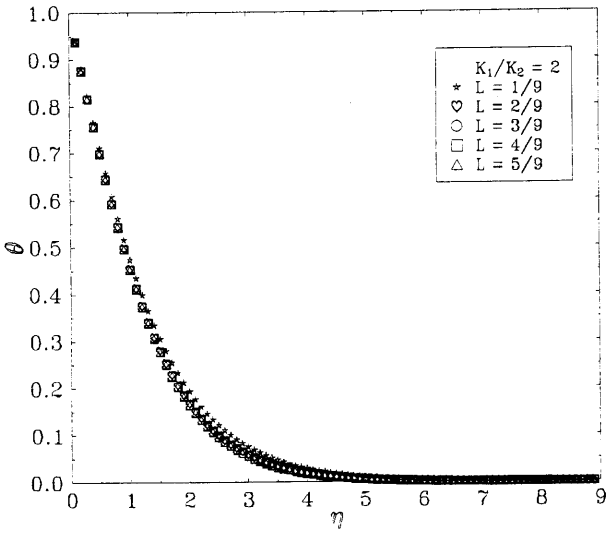

Fig. 2 Dimensionless temperature versus similarity variable for different porous layer length (L=1/9 to 5/9) with permeability ratio of K_1/K_2=2

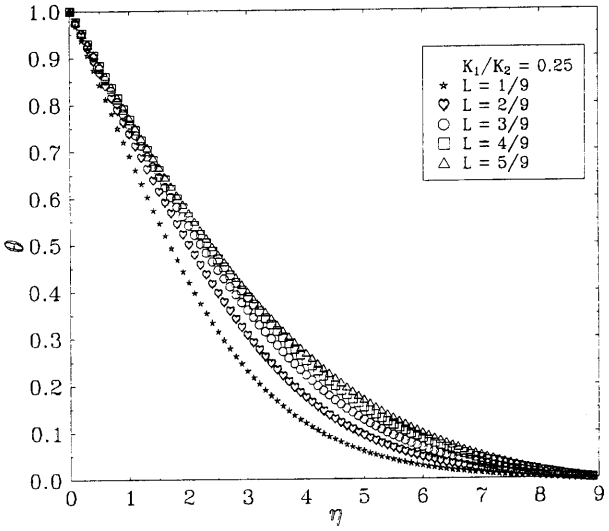

Fig. 4 Dimensionless temperature versus similarity variable for different porous layer length (L=1/9 to 5/9) with permeability ratio of K_1/K_2=0.25

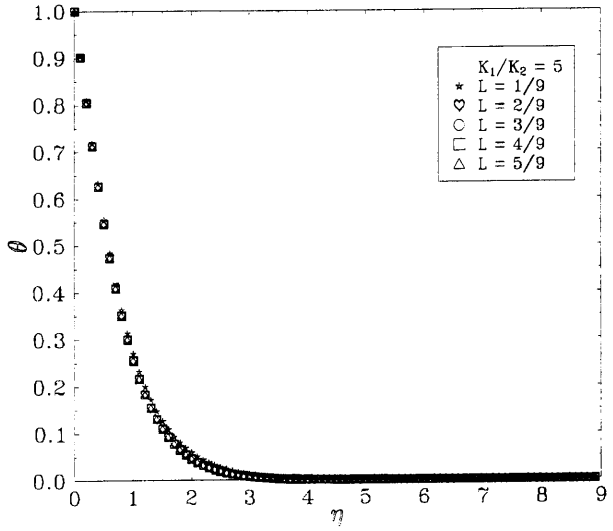

Fig. 3 Dimensionless temperature versus similarity variable for different porous layer length (L=1/9 to 5/9) with permeability ratio of K_1/K_2=5

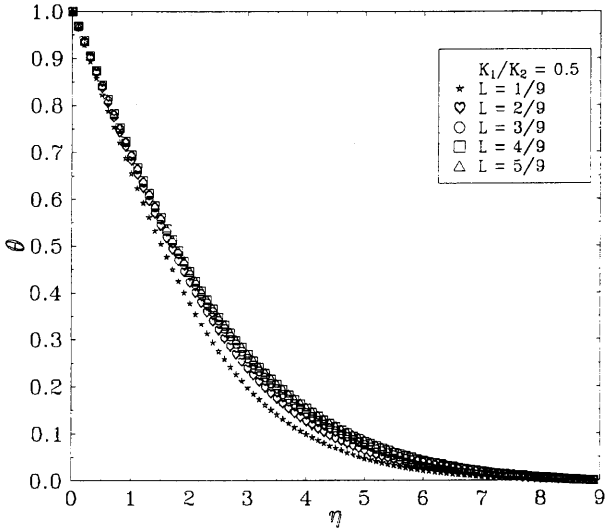

Fig. 5 Dimensionless temperature versus similarity variable for different porous layer length (L=1/3 to 5/9) with permeability ratio of K_1/K_2=0.50

found sufficiently far from the wall surface in all cases treated in this study.

For the case of constant surface temperature, the step size $\Delta\eta$=0.01 and η_∞=9 are taken. The results are shown in Figs. 2 - 5 for various porous layer lengths of different permeability values. These results have been compared to previous studies of Newtonian constant porosity case. It is found to be in a good agreement as shown in Table 1. Figures 2 and 3 show the dimensionless temperature versus the similarity variable η for different porosity layer length (L=1/9 to 5/9η) for the permeability ratio of 2 and 5 (i.e. K_1/K_2=2, and 5), respectively. If the permeability ratio is greater than one, the temperature variation comes to be constant when the porosity layer length increases. Namely, the thermal boundary layer do not effected by increasing the porosity layer length. In other words, the thermal boundary layer thickness becomes smaller than the specified porous layer length (L). Figures 4 and 5 show again the dimensionless temperature versus the similarity variable η, but for the permeability ratios of 0.25 and 0.5 (i.e. K_1/K_2=0.25, and 0.5), respectively. It is observed that the dimensionless temperature variation gets fewer as the porous layer length increases.

An interesting observation can be made in Fig. 6 in which Nusselt number versus the porous layer length is illustrated. While Fig. 6 shows that 0.2η is

Table 1 Dimensionless temperature distribution for Newtonian constant porosity medium (i.e. $K_1/K_2=1$)

	Ref. [2] Study	Present Study
η	$f'=\theta=u^*$	$f'=\theta=u^*$
0.000	1.00000	1.00000
1.000	0.58722	0.586922
4.000	0.06643	0.065348
7.000	0.00624	0.004878

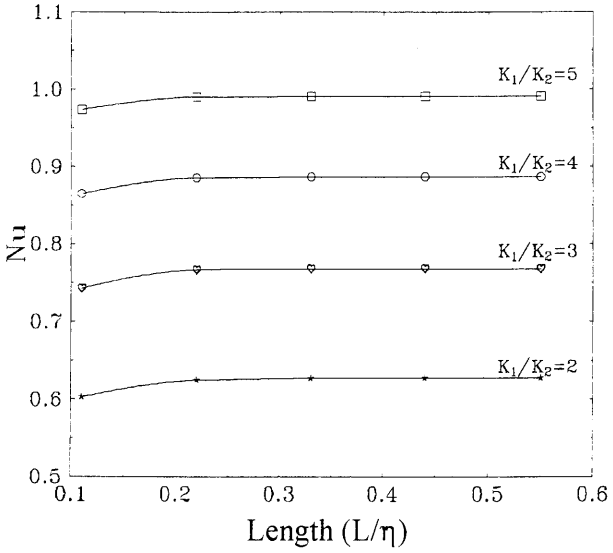

Fig. 6 Nusselt number versus porous layer length for permeability ratio >1

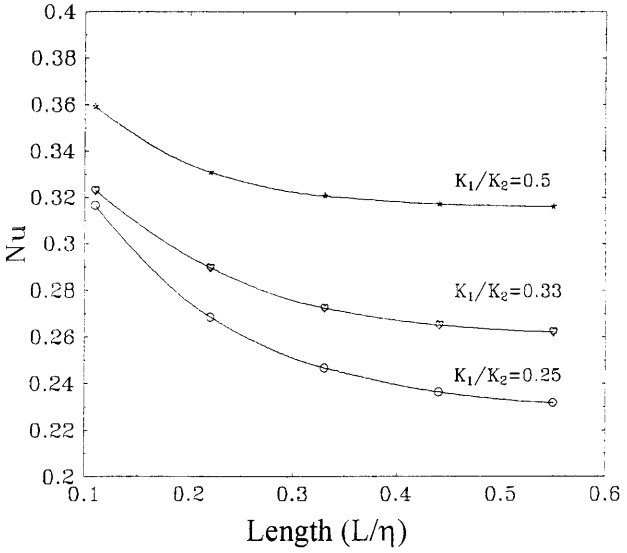

Fig. 7 Nusselt number versus porous layer length for permeability ratio <1

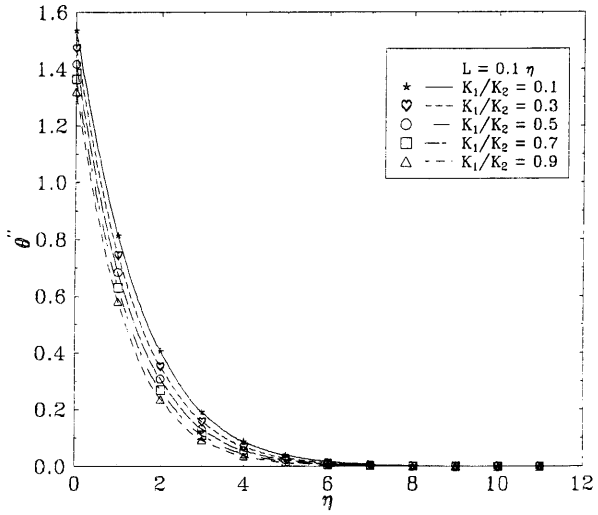

Fig. 8 Dimensionless temperature versus similarity variable for different permeability ratios of $K_1/K_2=0.1$ to 0.9 and porous layer thickness of $L=0.1\eta$

satisfactory to get Nusselt number to its constant value, this gives the impression that it is valuable to use a high permeability ratio layer in the range of 0.2η to get higher heat transfer rate instead of using constant permeability medium. Figure 7 shows Nusselt number versus layer length for permeability ratios less than one, and it indicates the large effect of using permeability ratio less than one in the reduction of Nusselt number values.

In the case of constant heat flux, the resulted nonlinear ordinary differential equations (i.e. Eqs. (41), (42), and (43)) with the boundary conditions (i.e. Eqs. (44), and (45)) are solved numerically with step size $\Delta\eta=0.01$ and $\eta_\infty=12$. The problem is analyzed in terms of the plate surface temperature with respect to the thickness of the first porous layer, and the permeability ratios (i.e. K_1/K_2) of the porous layers. The results are shown in Figs. 8 through 14 for variable porous layer thickness of different permeability values. Figures 8 and 9 show the dimensionless temperature versus the similarity variable η for different porous layer length ($L=0.1\eta$ and 0.4η), and for various permeability ratios, ($K_1/K_2=0.1$ to 0.9). It is clear that, as the porous layer length increases in case of the permeability ratio is less than one, the excess surface temperature increases and a lower dimensionless temperature variation is achieved. Figures 10 and 11 show again the dimensionless temperature versus the similarity variable η, but for the permeability ratios of $K_1/K_2=2$, 3, 4 and 5. It is observed that, the dimensionless temperature variation gets steeper as the porous layer length increases. In the Figs. 12 and 13, the dimensionless excess surface temperature versus the porous layer length is illustrated. Figure 12 shows that 0.2η is satisfactory to get the excess surface temperature to its constant value. This gives the

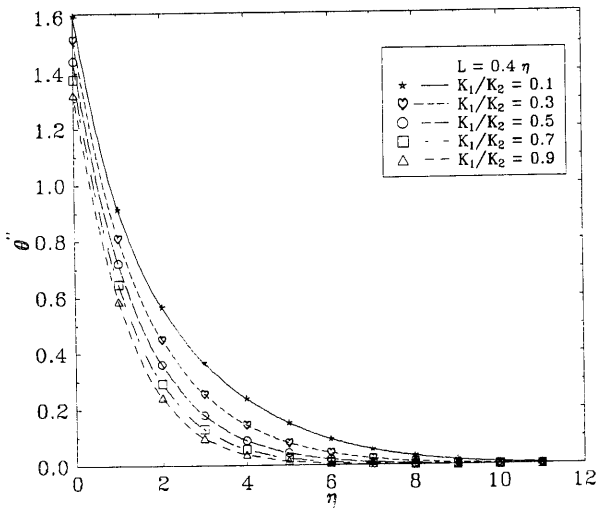

Fig. 9 Dimensionless temperature versus similarity variable for different permeability ratios of $K_1/K_2=0.1$ to 0.9 and porous layer thickness of $Q=0.4\eta$

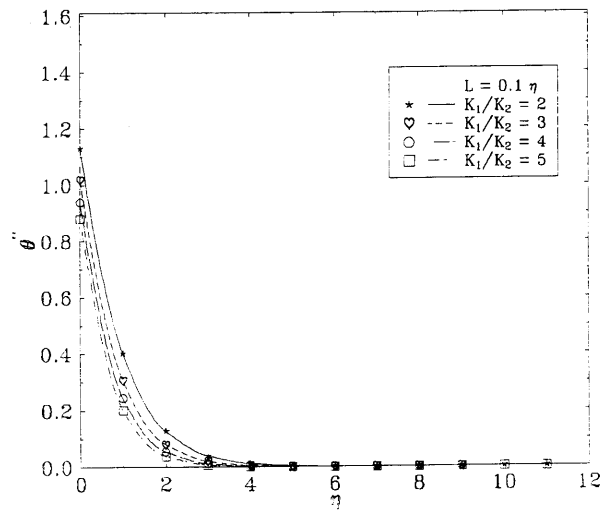

Fig. 10 Dimensionless temperature versus similarity variable for different permeability ratios of $K_1/K_2=$ 2 to 5 and porous layer thickness of $L=0.1\eta$

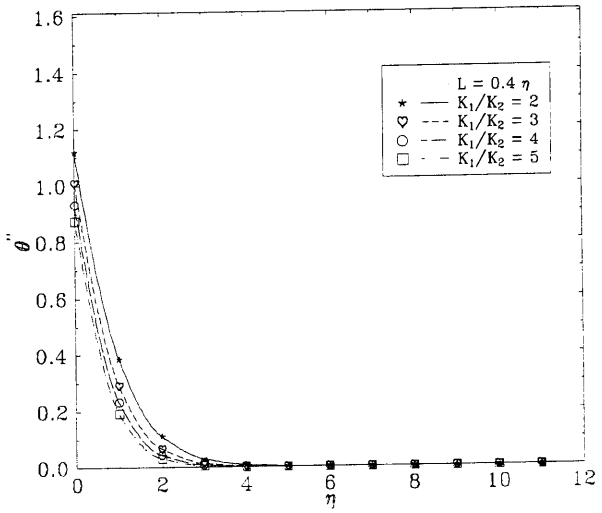

Fig. 11 Dimensionless temperature versus similarity variable for different permeability ratios of $K_1/K_2=$ 2 to 5 and porous layer thickness of $L=0.4\eta$

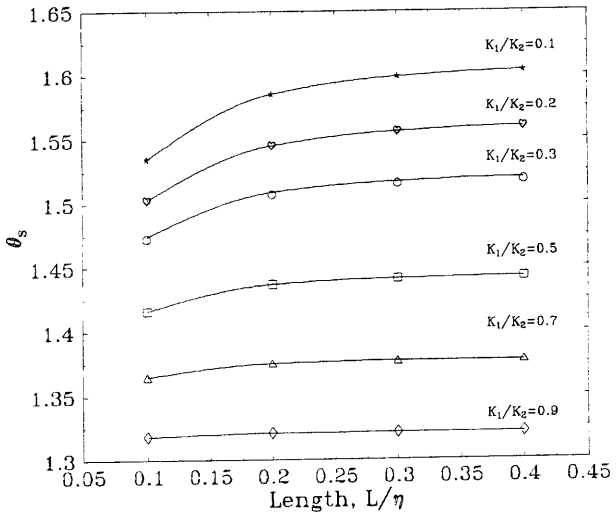

Fig. 12 Dimensionless excess surface temperature versus porous layer thickness for permeability ratio <1

impression that it is valuable to use a high permeability layer in the range of 0.2η to get higher heat transfer rate instead of using constant permeability medium. Figure 13 shows the excess surface temperature versus layer length for permeability ratios less than one. This figure indicates that as the permeability ratio decreases, the excess surface temperature increases. Figure 14 shows the excess surface temperature versus the permeability ratio for different porous layer length. It shows that decreasing the permeability ratio increases the excess surface temperature where at high permeability porous layer length grater than 0.2η the excess surface temperature for the same permeability ratio comes to be almost constant.

4. Conclusion

In this study, the effects of double layer porous medium on the free convection flow along vertical plate embedded in this porous medium are investigated for two cases: constant surface temperature, and constant heat flux. The results are obtained for different permeability ratios (i.e. K_1/K_2), and layer length, L. If the permeability ratio is taken 1, it means that two layers are the same, and it is constant permeability porous medium. For this case, the result is compered with the previous studies, and it is found that they are in good agreement. The results show that, as the porosity layer length increases for the permeability ratio greater than one the temperature

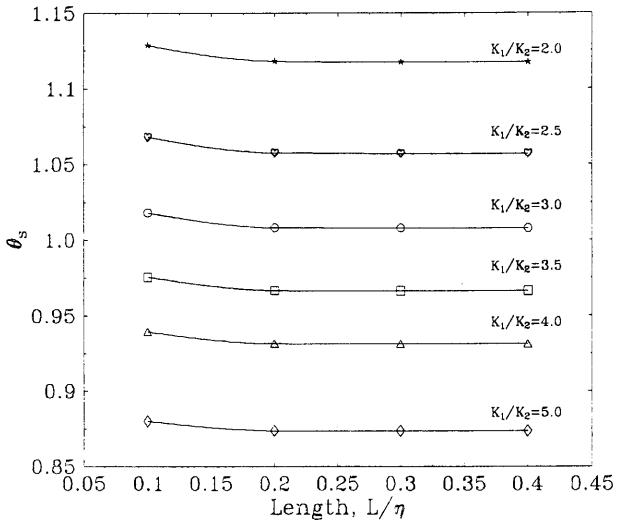

Fig. 13 Dimensionless excess surface temperature versus porous layer thickness for permeability ratio >1

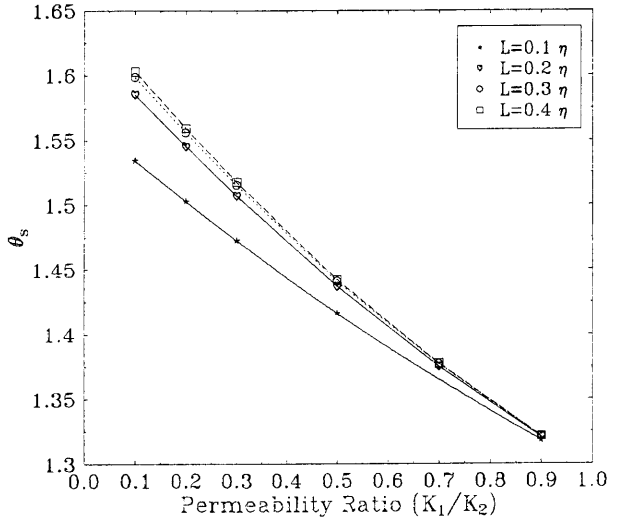

Fig. 14 Dimensionless excess surface temperature versus permeability ratio for different porous layer thicknesses

variation comes to be constant, whereas for the permeability ratios less than one the temperature variation gets slower as the porous layer length increases. Noting that permeability ratio is greater than one tend to increase Nusselt number, it was noted also that 0.2η is satisfactory to get Nusselt number to its constant value. This gives the impression that it is valuable to use a high permeability ratio layer in the range of 0.2η to get higher heat transfer rate instead of using constant permeability medium.

In the case of constant heat flux, the results are also obtained for different permeability ratios, and layer length. The results show that, as the porous layer length increases, the excess surface temperature increases for the permeability ratio less than one, and decreases for the permeability ratio greater than one. It was noted also that for permeability ratios that are greater than 1, 0.2η is satisfactory to get the excess surface temperature to its constant value. This gives the impression that it is valuable to use a high permeability ratio layer in the range of 0.2η to get higher heat transfer rate instead of using constant permeability medium.

In general, the results showed that using variable permeability is advantageous to obtain higher heat transfer rate instead of using single layer porous medium. In an engineering application, this result is important in the design of solar heating convectors that uses porous medium.

References

(1) Dharmadhikari, R.V. and Kale, D.D., Flow of Non-Newtonian Fluids Through Porous Media, Chem. Engng.Sci., Vol. 40, No. 3 (1985), pp. 527-529.

(2) Chen, H. and Chen, C., Free Convection Flow of Non-Newtonian Fluids along a Vertical Plate Embedded in a Porous Medium, Journal of Heat Transfer, Vol. 110 (1988), pp. 257-260.

(3) Nakayama, A. and Koyama, H., Bouyancy-Induced Flow of Non-Newtonian Fluids over a Non-Isothermal Body of Arbitrary Shape in a Porous Medium, Applied Scientific Research, Vol. 48 (1991), pp. 55-70.

(4) Mehta, K.N. and Narasimha, K., Buoyancy-Induced Flow of Non-Newtonian Fluids in a Porous Medium Past a Vertical Flat Plate with Non-Uniform Surface Heat Flux, Int. Journal of Engineering Science, Vol. 32 (1994), pp. 297-302.

(5) Ress, D.A.S., The Effect of Inertia on Free Convection from a Horizontal Surface Embedded in a Porous Medium, Int. J. Heat Mass Transfer, Vol. 39, No. 16 (1996), pp. 3425-3430.

(6) Nield, A.D. and Bejan, A., Convection in Porous Medium, (1992), Spring-Verlag New York Inc.

(7) Argento, C. and Bouvard, D., A Ray Tracing Method for Evaluating the Radiative Heat Transfer in Porous Medium, Int. J. Heat Mass Transfer, Vol. 39, No. 15 (1996), pp. 3175-3180.

(8) Bejan, A., Convection Heat Transfer, (1984), A Wiley-Interscience Publication, New York.